



**US Army Corps
of Engineers®**
Engineer Research and
Development Center



Aquatic Nuisance Species Research Program

Regional Analysis of Lake and Reservoir Water Quality with Multispectral Satellite Remote Sensing Images

Min Xu, Hongxing Liu, Richard A. Beck, Molly K. Reif, Erich B. Emery, November 2019
and Jade L. Young



The U.S. Army Engineer Research and Development Center (ERDC) solves the nation's toughest engineering and environmental challenges. ERDC develops innovative solutions in civil and military engineering, geospatial sciences, water resources, and environmental sciences for the Army, the Department of Defense, civilian agencies, and our nation's public good. Find out more at www.erd.c.usace.army.mil.

To search for other technical reports published by ERDC, visit the ERDC online library at <http://acwc.sdp.sirsi.net/client/default>.

Regional Analysis of Lake and Reservoir Water Quality with Multispectral Satellite Remote Sensing Images

Min Xu and Hongxing Liu

*Department of Geography
The University of Alabama
513 University Blvd
Tuscaloosa, AL 35487*

Richard A. Beck

*Department of Geography and Geographic Information Science
University of Cincinnati
Cincinnati, OH 45221*

Molly K. Reif

*U.S. Army Corps of Engineers, ERDC, JALBTCX
7225 Stennis Airport Rd
Kiln, MS, 39556*

Erich B. Emery

*U.S. Army Corps of Engineers, Great Lakes and Ohio River Division
550 Main Street
Cincinnati, OH 45202*

Jade L. Young

*U.S. Army Corps of Engineers, Louisville District, Water Quality
Louisville, KY 40202*

Final report

Approved for public release; distribution is unlimited.

Prepared for Aquatic Nuisance Species Research Program
US Army Engineer Research and Development Center
Environmental Laboratory
Vicksburg, MS 39180-6199

Under Funding Account Code 96 X 3123; AMSCO Code 008284

Abstract

In this research, a time-series of multispectral images acquired by Landsat 8 and Sentinel-2 satellites during 2013-2017 was combined with in situ water quality measurements to examine and analyze the spatial pattern and temporal variation of lake and reservoir water quality in the Ohio/Kentucky/Indiana region within the Louisville District, United States Army Corps of Engineers. Reflectance values at the sampling sites for each lake were used with the in situ data collected within a 7-day time window of satellite overpass to construct empirical models to estimate water quality parameters, including turbidity, Secchi depth, and chlorophyll-a. The analysis indicated that Sentinel-2 outperformed Landsat 8 for retrieving water quality parameters, especially for chlorophyll-a. Due to the better spatial and temporal coverage of Landsat 8 for this tri-state region, the Secchi depth retrieved from the time-series Landsat 8 images was used to create lake trophic state index (TSI) maps in 2013, 2015, and 2017. It was observed that most lakes (~75%) in the study area were in mesotrophic or eutrophic classes in 2017 based on the TSI. From 2013 to 2017, the TSI range and standard deviation of lakes in Indiana region largely increased while the average TSI in this tri-state area varied slightly (<1.6%).

DISCLAIMER: The contents of this report are not to be used for advertising, publication, or promotional purposes. Citation of trade names does not constitute an official endorsement or approval of the use of such commercial products. All product names and trademarks cited are the property of their respective owners. The findings of this report are not to be construed as an official Department of the Army position unless so designated by other authorized documents.

Contents

Abstract.....	ii
Figures and Tables.....	iv
Preface.....	v
1 Introduction.....	1
1.1 Background.....	1
1.2 Objective.....	3
1.3 Approach.....	3
2 Materials.....	4
2.1 Study area.....	4
2.2 Satellite data.....	6
2.3 Water truth data.....	10
3 Methods.....	12
3.1 Preprocessing of multispectral satellite images.....	12
3.2 Water quality parameter retrieval models.....	13
3.3 Trophic state index (TSI) calculation.....	13
4 Results.....	15
4.1 Results from Landsat 8 data.....	15
4.2 Results from Sentinel-2 data.....	19
4.3 Spatial pattern of lakes' trophic state.....	21
4.4 Temporal variability of lakes' trophic state.....	24
4.5 TSI in individual lakes.....	26
5 Discussion.....	28
6 Conclusion.....	31
References.....	32
Acronyms and Abbreviations.....	35
Report Documentation Page	

Figures and Tables

Figures

Figure 1. Landsat 8 paths and rows over the study area within the USACE Louisville District.	4
Figure 2. Sentinel-2 tiles over the study area.	5
Figure 3. Power relationship between turbidity (NTU) and Secchi depth (m).	11
Figure 4. Estimated turbidity (NTU), Secchi depth (m), and Chl-a ($\mu\text{g/L}$) from Landsat 8 data compared with <i>in situ</i> measurements using the testing data set.	18
Figure 5. Estimated turbidity (NTU), Secchi depth (m), and Chl-a ($\mu\text{g/L}$) from Sentinel-2 data compared with <i>in situ</i> measurements using the testing data set.	20
Figure 6. TSI of lakes in September 2017.	22
Figure 7. TSI of lakes in September 2013.	24
Figure 8. TSI of lakes in September 2015.	25
Figure 9. TSI of Brookville Lake, Rough River Lake, and Barren River Lake in September 2013, September 2015, and September 2017 (mean TSI shown in the right bottom corner).	27

Tables

Table 1. Twelve USACE lakes in the study area.	6
Table 2. Band configurations and spatial resolutions of Landsat 8 OLI sensor.	7
Table 3. Band configurations and spatial resolutions of Sentinel-2 MSI sensor.	8
Table 4. Satellite images and lakes sampled within 7 days of satellite overpass.	9
Table 5. Total number of match-up pairs and size of training and testing sets for retrieving turbidity (NTU), Secchi depth (m), and Chl-a ($\mu\text{g/L}$) from Landsat 8 or Sentinel-2 image data.	15
Table 6. Trophic state classification of 845 lakes in the study area.	23
Table 7. Summary of lakes' TSI in September 2017.	23
Table 8. TSI and classification of 12 USACE lakes in September 2017.	23
Table 9. Summary of lakes' TSI from different years.	26
Table 10. TSI and classification of 12 USACE lakes from different years.	26

Preface

This study was conducted for the Aquatic Nuisance Species Research Program (ANSRP), under Funding Account Code 96 X 3123; AMSCO Code 008284. The ANSRP is sponsored by Headquarters, U.S. Army Corps of Engineers, and is assigned to the U.S. Army Engineer Research and Development Center (ERDC) under the purview of the Environmental Laboratory (EL), Vicksburg, MS. The ANSRP Program Manager is Dr. Linda Nelson.

Appreciation is expressed to Dr. Glenn Suir and Mr. Sam Jackson for their review of this manuscript and also to Dr. Richard Beck, University of Cincinnati, and Dr. Hongxing Liu, The University of Alabama.

This report was prepared under the general supervision of Mr. Mark Graves, Chief, Environmental Systems Branch; Mr. Mark D. Farr, Chief, Ecosystem Evaluation and Engineering Division; and Dr. Ilker R. Adiguzel, Director, EL.

At the time of the publication of this report, COL Teresa A. Schlosser was the Commander of ERDC, and Dr. David W. Pittman was the Director.

1 Introduction

1.1 Background

Inland water bodies are sensitive and fragile environments, which are increasingly threatened by climate change, anthropogenic activities, and other natural stressors (Blondeau-Patissier et al. 2014). The need for sustainable water supplies for human consumption, agriculture, industry, and other economic activities necessitates the monitoring of inland water quality. For accurate assessment and effective management of inland lakes, it is important to have the spatial and temporal view of lake water quality, allowing managers to take into account not only differences among lakes, but also the changes of lakes through time (Kloiber et al. 2002a). Conventional in situ sampling methods for collecting water quality parameters are time consuming, expensive, and limited in spatial coverage and sampling density. The synoptic view of water quality is thus not practical with traditional sampling methods (Kloiber et al. 2002b). Satellite-based remote sensing has been used as the most cost-effective and practical means of gathering information needed for regional water quality assessments because it is able to provide synoptic, frequent, and consistent observations on the water quality of lakes (Ritchie et al. 2003).

Water clarity and trophic state are two related water quality characteristics that are measurable from remotely sensed imagery (Olmanson et al. 2011). Water clarity is commonly evaluated in terms of turbidity or Secchi depth. Turbidity as the surrogate for total suspended matter is a direct measurement of light scattering properties of water and is inversely related to water clarity (Dogliotti et al. 2015). Secchi depth is also widely used as the proxy variable for water clarity. It is measured by slowly lowering a standardized black and white disk (Secchi disk) into the water and finding the depth at which the disk ceases to be visible from the surface (Chen et al. 2007). Many studies suggest a strong power relationship between turbidity and Secchi depth (Effler 1988; Harrington et al. 1992).

Trophic state is normally evaluated in terms of total phosphorus, chlorophyll-a (Chl-a), or Secchi depth. Trophic state index proposed by Carlson (1977) is frequently used to classify the water bodies into different trophic states such as oligotrophic, mesotrophic, eutrophic,

supereutrophic, or hypereutrophic, to rate the biological conditions of water. Oligotrophic lakes usually have deep clear water with low nutrients and low algae biomass (Dodds et al. 1998). Mesotrophic lakes have a medium amount of nutrients and have clear water with some algal blooms in the summer. Eutrophic lakes have high biological productivity due to high total nutrients. Frequent algal blooms occur in eutrophic lakes. Hypereutrophic lakes with excessive nutrients are characterized by severe nuisance algal blooms and low water clarity. Supereutrophic lakes have intermediate characteristics between eutrophic and hypereutrophic lakes. Except for total phosphorus, water quality parameters including Chl-a, turbidity, and Secchi depth can be inferred from satellite imagery because of their optical properties. The water quality parameters and derived trophic state index have been used by regulatory and resource management agencies to guide water management and public safety decisions (El-Serehy et al. 2018; Olmanson et al. 2015).

Satellite imagery has been used for regional-scale measurements of lake water quality for the past few decades. Satellite sensors suitable for water quality assessments of lakes at a regional scale should have the appropriate spatial resolution (5-50 m), regular and frequent revisits (preferably at least weekly), appropriate spectral bands (sensitive spectral responses to water quality constituents), and should be inexpensive or freely available (Olmanson et al. 2015). Landsat sensors, including Landsat Multispectral Scanner, Landsat Thematic Mapper, Landsat Enhance Thematic Mapper Plus, and Landsat 8 have been extensively used for regional water clarity studies for the states of Minnesota, Maine, Michigan, and Wisconsin (Fuller et al. 2004; Fuller and Minnerick 2007; Kloiber et al. 2002a; Kloiber et al. 2002b; Martin et al. 1983; McCullough et al. 2012; Olmanson et al. 2008; Olmanson et al. 2016). To date, no regional study has addressed water quality issues for the Ohio/Kentucky/Indiana region. Landsat imagery is used primarily for terrestrial applications. The placement and bandwidth of their spectral bands may not be suitable for the accurate retrieval of Chl-a concentration (Olmanson et al. 2015). Recently launched European Space Agency Sentinel-2 satellites are expected to improve and expand the capabilities in regional assessment of water quality due to the improved spectral band configuration and enhanced spatial and temporal resolution.

1.2 Objective

This study examines the spatial pattern and temporal variability of lake water quality in the Ohio/Kentucky/Indiana region within the Louisville District, United States Army Corps of Engineers (USACE), by combining the time-series satellite imagery from Landsat 8 and Sentinel-2, spanning 2013-2017. Historical in situ water quality data from multiple sources were used in the calibration of water quality remote sensing models. The water quality parameter retrieval models calibrated from Landsat 8 and Sentinel-2 data were evaluated and compared, and the trophic state was used as an indicator of water quality for the regional assessment. In the following sections, there is first an introduction of the case study area and a description of relevant data sets. Then, there is a presentation of the empirical algorithms for retrieving turbidity, Secchi depth, and Chl-a concentration in inland lakes from satellite imagery. Next, the estimated water quality parameters were used to evaluate and classify the trophic state of lakes in the study area. Finally, there is a discussion of the spatial pattern and temporal variability of trophic state in lakes, followed by some conclusions.

1.3 Approach

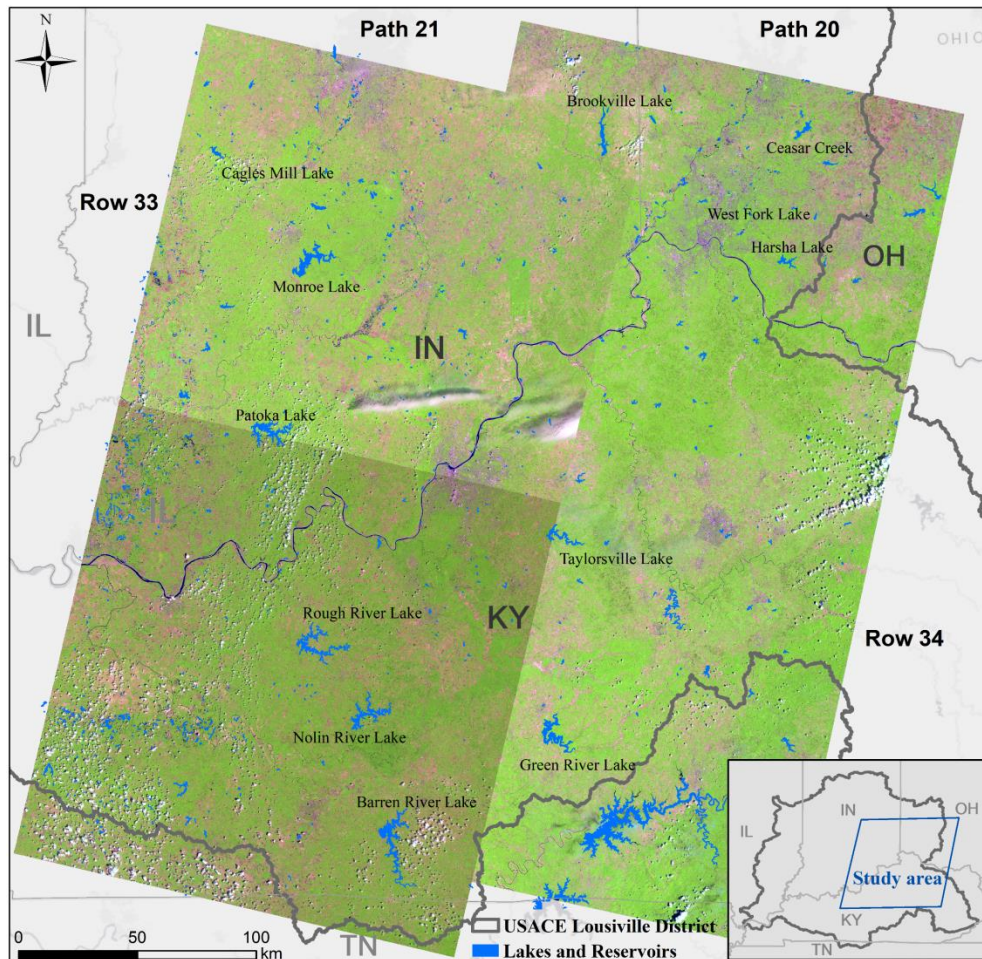
The approach is addressed in Chapter 3, Methods.

2 Materials

2.1 Study area

The USACE Louisville District, established in 1886, consists of a five-state area of Illinois, Indiana, Kentucky, Ohio, and Tennessee (<https://www.lrl.usace.army.mil/>) (Figure 1). The civil works mission of Louisville District, with an area of responsibility of approximately 190,000 km², aims to develop, protect, and restore the water and land resources in the defined region (<https://www.lrl.usace.army.mil/Missions/Civil-Works/>). Twenty flood-risk reduction lakes or reservoirs in this district constructed by the USACE are assessed annually by the Louisville District Water Quality Team for the monitoring and evaluation of water quality conditions.

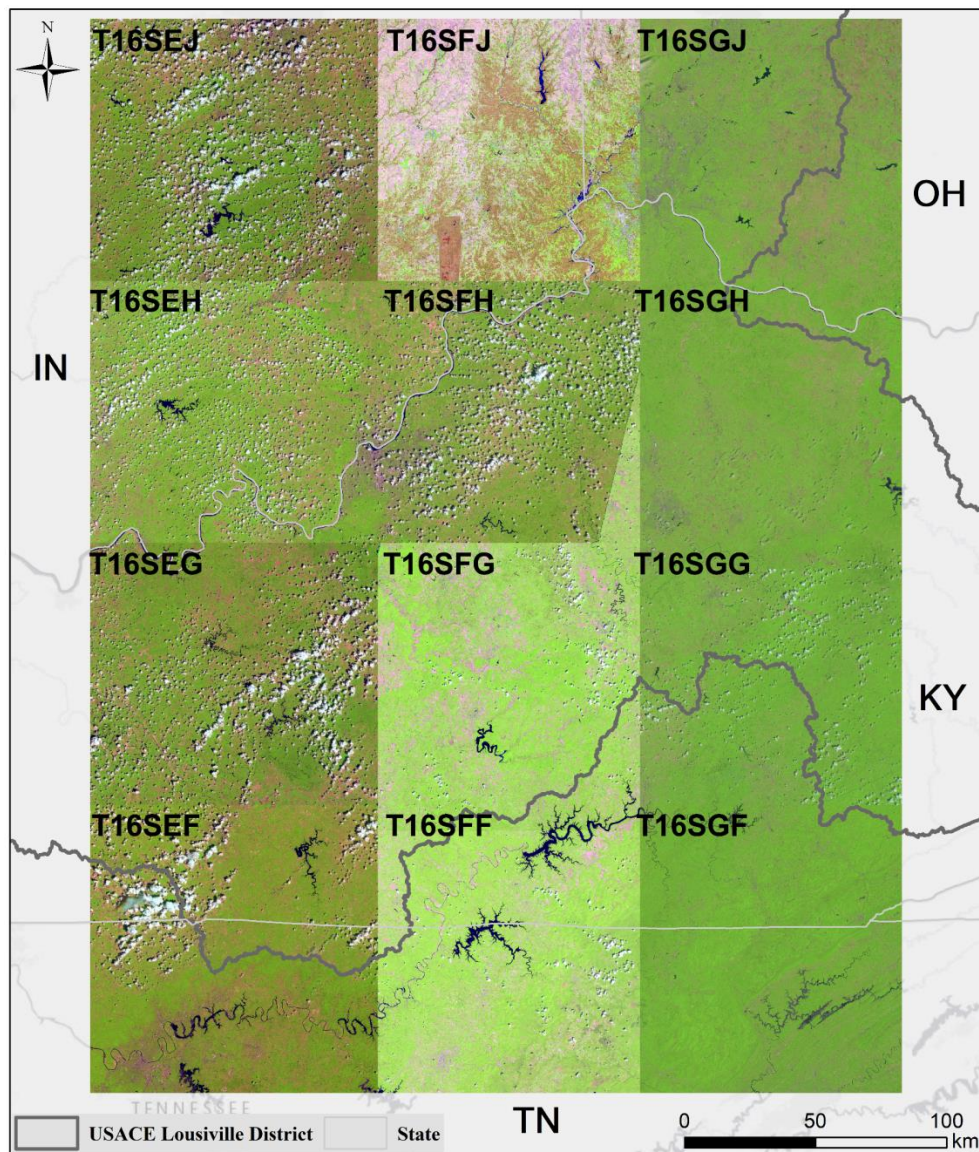
Figure 1. Landsat 8 paths and rows over the study area within the USACE Louisville District.



The 20 lakes or reservoirs include 8 in Kentucky, 8 in Indiana, and 4 in Ohio. They provide flood control, water supply and water quality control, and recreational opportunities, including fishing and hunting, boating, and swimming.

The study area is a tri-state region of Ohio, Kentucky, and Indiana within the USACE Louisville District, covered by Landsat 8 paths 20-21, rows 33-34 (Figure 1) or Sentinel-2 tiles T16SEJ-T16SEF, T16SFJ-T16SFF, and T16SGJ-T16SGF (Figure 2).

Figure 2. Sentinel-2 tiles over the study area.



Within the study area, lakes greater than 90,000 m² were used for analysis. The selection of lakes was based on the lake and reservoir masks in the National Hydrography Dataset (<https://www.usgs.gov/core-science-systems/ngp/national-hydrography>). Among the 845 studied lakes and reservoirs, 5 lakes in Kentucky, 4 lakes in Indiana, and 3 lakes in Ohio (Table 1) are the 12 USACE lakes located in the case study area (Figure 1).

Table 1. Twelve USACE lakes in the study area.

State	Lakes
KY	Barren River Lake
	Green River Lake
	Nolin River Lake
	Rough River Lake
	Taylorsville Lake
IN	Brookville Lake
	Cagles Mill Lake
	Monroe Lake
	Patoka Lake
OH	Caesar Creek Lake
	West Fork Lake
	Harsha Lake

2.2 Satellite data

Remote sensing data used in this study include Landsat 8 and Sentinel-2 multispectral images acquired during 2013-2017. Landsat 8, launched in 2013, carries an Operational Land Imager (OLI) and a Thermal Infrared Sensor (TIRS). The OLI sensor has nine spectral bands in the visible and near infrared (VNIR) and shortwave infrared (SWIR) portions of the spectrum (Table 2). The two thermal bands (TIRS), measuring surface temperature, are not used in this study. Landsat 8 has a revisit cycle of 16 days. Compared with previous Landsat sensors, Landsat 8 OLI has an improved radiometric resolution of 12 bits and better signal-to-noise ratio (SNR). Landsat 8 Level 1TP (L1TP) data products were obtained from United States Geological Survey, EarthExplorer (<https://earthexplorer.usgs.gov/>). The L1TP products are full scenes (170 km × 185 km) of top-of-atmosphere

(TOA) digital numbers in Universal Transverse Mercator (UTM) map projection with reference to World Geodetic System 84 (WGS84) datum.

Table 2. Band configurations and spatial resolutions of Landsat 8 OLI sensor.

Band ID	Description	Wavelength (nm)	Spatial Resolution (m)
B1	Coastal aerosol	430-450	30
B2	Blue	450-510	30
B3	Green	530-590	30
B4	Red	640-670	30
B5	NIR	850-880	30
B6	SWIR 1	1570-1650	30
B7	SWIR 2	2100-2290	30
B8	Panchromatic	500-680	15
B9	Cirrus	1360-1380	30

The Sentinel-2 remote sensing system consists of two identical satellites: Sentinel-2A launched in 2015 and Sentinel-2B launched in 2017. The constellation of the two satellites provides a revisit time of 5 days at the equator. Flying at an altitude of 786 km, Sentinel-2 has a ground swath of 290 km. Sentinel-2 carries a multispectral instrument (MSI) with spectral bands summarized in Table 3 (Drusch et al. 2012). The sensor's radiometric resolution is 12-bit. The unique combination of high spatial and temporal resolution, wide field of view, high radiometric sensitivity and SNR, and good spectral configuration makes Sentinel-2 MSI a valuable sensor for assessing and monitoring the water quality of inland lakes (Xu et al. 2018). Sentinel-2 Level 1C (L1C) products in Standard Archive Format for Europe format were obtained from the Copernicus Open Access Hub (<https://scihub.copernicus.eu/>). The L1C products were 100 km tiles of TOA reflectance in UTM/WGS84 projection. Both Landsat 8 L1TP and Sentinel-2 L1C images were atmospherically corrected to the bottom-of-atmosphere (BOA) reflectance to remove the atmospheric influence.

Table 3. Band configurations and spatial resolutions of Sentinel-2 MSI sensor.

Band ID	Description	Central Wavelength (nm)		Spatial Resolution (m)
		Sentinel-2A	Sentinel-2B	
B1	Coastal aerosol	442.7	442.2	60
B2	Blue	492.4	492.1	10
B3	Green	559.8	559.0	10
B4	Red	664.6	664.9	10
B5	Vegetation Red Edge	704.1	703.8	20
B6	Vegetation Red Edge	740.5	739.1	20
B7	Vegetation Red Edge	782.8	779.7	20
B8	NIR	832.8	832.9	10
B8a	Narrow NIR	864.7	864.0	20
B9	Water vapor	945.1	943.2	60
B10	SWIR – Cirrus	1373.5	1376.9	60
B11	SWIR	1613.7	1610.4	20
B12	SWIR	2202.4	2185.7	20

Landsat 8 and Sentinel-2 images taken during 2013-2017 that presented cloud cover less than 10% were identified. Among these satellite images, the ones containing lakes that were sampled within a 7-day time window of the satellite overpasses were selected. Field sampling data collected in such a time window have proven to be usable in previous studies (McCullough et al. 2012; Olmanson et al. 2008). The remotely sensed images after atmospheric correction and normalization were combined with in situ Global Positioning System stamped water quality sampling data to develop and assess the algorithms for retrieving turbidity, Secchi depth, and Chl-a concentration in the lakes.

Table 4 lists Landsat 8 and Sentinel-2 images used in this study for remote retrieval of lake water quality parameters. Those include 24 Landsat 8 L1TP images and 11 Sentinel-2 L1C products. Considering the cloud coverage constraint and availability of in situ water quality data, suitable images for the analysis span the period from May 1, 2013 to November 20, 2017, with most images acquired in August and September.

Table 4. Satellite images and lakes sampled within 7 days of satellite overpass.

(a) Landsat 8			
Path	Row	Acquisition date	Lakes
21	34	9/17/2017	Barren River
21	34	8/27/2015	Barren River, Nolin River
21	34	8/5/2013	Barren River, Nolin River
21	34	10/19/2017	Nolin River
21	34	3/9/2017	Nolin River
21	34	8/29/2016	Nolin, Rough River
21	34	9/22/2013	Rough River
21	33	8/5/2013	Jericho
21	33	5/1/2013	Jericho
21	33	10/8/2013	Cagles Mill
21	33	8/29/2016	Patoka
21	33	11/20/2017	Brookville
20	33	9/26/2017	Brookville
20	33	9/10/2017	Brookville
20	33	8/9/2017	Brookville
20	33	6/6/2017	Brookville, Caesar Creek, Harsha, West Fork
20	33	10/9/2016	Caesar Creek
20	33	9/7/2016	Harsha, West Fork
20	33	9/18/2014	Harsha, West Fork
20	33	9/21/2015	Waynoka
20	34	11/21/2014	Herrington
20	34	10/9/2016	Green River
20	34	9/7/2016	Green River
20	34	9/23/2016	Taylorsville

Table 4. Continued.

(b) Sentinel-2		
Tile	Acquisition date	Lakes
T16SFJ	8/3/2017	Brookville
T16SFJ	7/7/2017	Brookville
T16SFJ	5/15/2017	Brookville
T16SFJ	5/8/2017	Brookville
T16SEG	5/8/2017	Nolin River
T16SEG	3/9/2017	Nolin River
T16SEF	9/25/2017	Barren River
T16SEF	10/6/2015	Barren River
T16SGJ	10/7/2016	Caesar Creek
T16SEJ	9/5/2017	Cagles Mill
T16SFG	8/28/2016	Green River

2.3 Water truth data

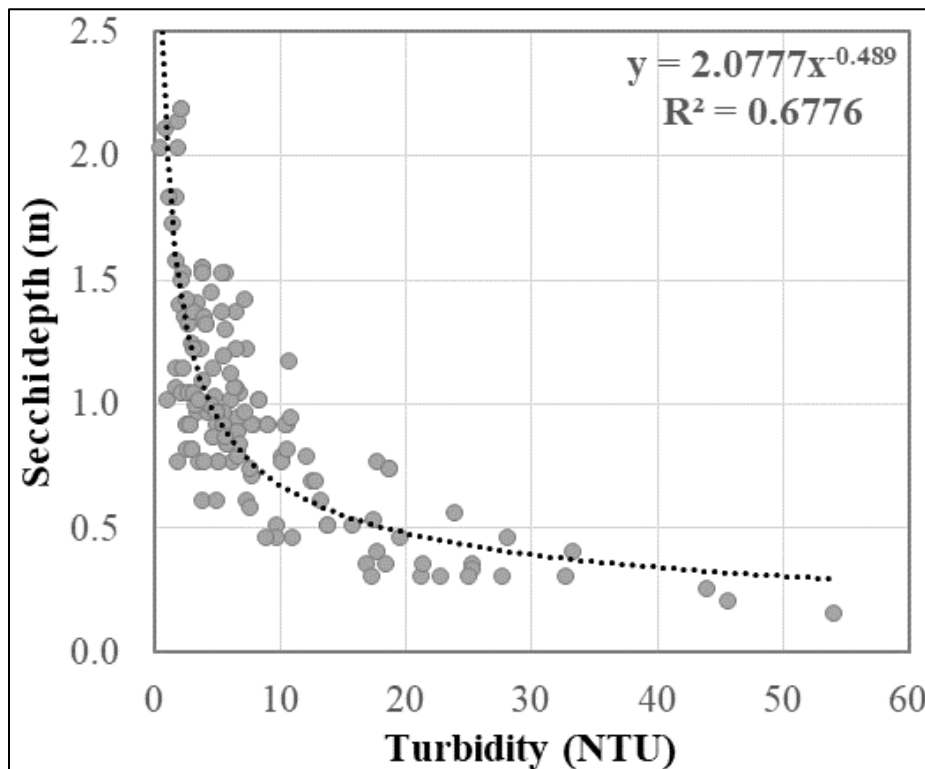
This research uses in situ water quality data collected by the USACE Louisville District Water Quality Team (<https://www.lrl.usace.army.mil/Missions/Civil-Works/Water-Information/Water-Quality/>) and water quality data retrieved from the United States Environmental Protection Agency (USEPA) Water Quality Portal (<https://www.epa.gov/waterdata/water-quality-data-wqx>). The USACE Louisville District Water Quality Team is responsible for the monitoring and assessment of biological, physical, and chemical properties of the 20 USACE lakes mentioned previously. The USEPA Water Quality Portal is currently the nation's largest source for sharing water quality data from approximately 400 federal, state, tribal, and other agencies and groups. Both data sets provide in situ measurements of water quality parameters, including water temperature (°C), dissolved oxygen (milligrams per liter), pH, turbidity (nephelometric turbidity units [NTU]), Secchi depth (meter), and chlorophyll concentration (micrograms per liter), which are used as the water truth data for the development and validation of water quality parameter retrieval models in the present study.

The water quality data for lakes in the study region that were sampled within 7 days of satellite overpasses were targeted and organized. After examining the satellite imagery, water quality data collected at locations near land features (e.g., shorelines and bridges) or in clouds or shadows

were discarded to avoid mixed pixels. This pre-processing step resulted in 123 water quality records of 14 lakes for Landsat 8 and 36 water quality records of 6 lakes for Sentinel-2.

Based on the water truth data, the Secchi depth measurements of lakes in this study area ranged from 0.15 to 2.18 m with an average depth of 0.97 m. The minimum, maximum, and mean values of turbidity are respectively 0.5, 54.0, and 8.6 NTU, respectively. As expected, there is a strong relationship between the measured turbidity and Secchi depth: $y=2.0777x^{-0.489}$, with $R^2 = 0.68$ (Figure 3). The Chl-a concentrations varied from 2.5 to 63.1 $\mu\text{g/L}$, and the average concentration was 12.6 $\mu\text{g/L}$.

Figure 3. Power relationship between turbidity (NTU) and Secchi depth (m).



3 Methods

3.1 Preprocessing of multispectral satellite images

As a considerable amount of the radiation received by a satellite sensor is originated from the atmosphere rather than the water surface, atmospheric correction is critical for accurate retrieval of water quality parameters from satellite imagery (Vidot and Santer 2005). Removing atmospheric effects is especially important when time series images are involved. Atmospheric correction converts TOA signal (Landsat 8 L1TP products or Sentinel-2 L1C images) to BOA reflectance (surface reflectance) with the atmospheric influence removed.

In this study, radiometric calibration, atmospheric correction, and between-image normalization were performed on both Landsat 8 and Sentinel-2 images. Landsat 8 L1TP images were calibrated to TOA radiance in units of $\mu\text{W}/(\text{cm}^2 * \text{sr} * \text{nm})$ in Environment for Visualizing Images (ENVI) 5.3 using the Radiometric Calibration function. Since the spatial resolutions of Sentinel-2 bands are different, the L1C products were resampled to 10 m pixel size using the nearest neighbor resampling method in the Sentinel Application Platform (SNAP) 6.0. The Reflectance to Radiance processor in SNAP was used to convert resampled L1C images from TOA reflectance to TOA radiance, and then Band Math function in ENVI 5.3 was used to scale the TOA radiance in units of $\mu\text{W}/(\text{cm}^2 * \text{sr} * \text{nm})$. Next, the processed Sentinel-2 images were converted to band-interleaved-by-line format based on the Convert Interleave module in ENVI 5.3.

The above procedures make Landsat 8 and Sentinel-2 images meet the input requirements for Fast Line-of-sight Atmospheric Analysis of Spectral Hypercubes (FLAASH) atmospheric correction method (Adler-Golden et al. 1998). Atmospheric correction of satellite images using the FLAASH software package in ENVI 5.3 was performed. This method has been widely applied to remove the atmospheric effect from remotely sensed imagery for estimating in-water constituents (Beck et al. 2016; Kutser et al. 2005; Watanabe et al. 2017; Xu et al. 2019). After atmospheric correction, some pseudo invariant features (e.g., large buildings and airport tarmacs) on the clearest image for each path or tile were used as the reference for normalizing the other images on the same path or tile. To

reduce noise, the satellite images after normalization were processed using a median filter with a 3×3 moving window in ENVI 5.3.

3.2 Water quality parameter retrieval models

Empirical algorithms that apply statistical regression techniques to determine the best-fit model between satellite bands (or band combinations) and water truth data have provided accurate and reliable retrieval of water quality parameters from remotely sensed imagery (Olmanson et al. 2011). Stepwise regression procedures have been widely used to model the empirical relationship (Olmanson et al. 2011; Olmanson et al. 2016). In this study, forward stepwise regression to develop the models to retrieve turbidity, Secchi depth, and Chl-a concentration from satellite images was utilized. Raw and log-transformed values of each water quality parameter as the dependent variables were adopted. Single bands, non-reciprocal band ratios, and band differences were used as the independent variables. Instead of employing preconceived notions concerning the best bands or band combinations for modeling the parameter of interest, all of them were entered and the stepwise regression method was used to identify the best ones by performing regression a number of times, each time adding the most correlated variable. To make the models accurate and compact, the models that had a good regression fit and included two independent variables were selected. The selected multiple regression model can be expressed as follows:

$$WQP \text{ or } \log_{10}(WQP) = a + b * BC_1 + c * BC_2 \quad (1)$$

where

WQP	=	water quality parameter of interest
BC_1, BC_2	=	selected explanatory variables
a, b, c	=	regression coefficients.

3.3 Trophic state index (TSI) calculation

The Carlson's TSI (Carlson 1977) is commonly used to classify the lakes' trophic status to rate the biological conditions of lakes. Three variables, including total phosphorus, Chl-a, or Secchi depth, can be used to calculate the Carlson TSI. In this study, TSI as an indicator of lake water quality was used. Based on the TSI values, the lakes in the study area were classified into different trophic states, and their spatial pattern and

temporal variability were analyzed. The equations to calculate TSI from Secchi depth or Chl-a are expressed as follows:

$$TSI = 60 - 14.41 * \ln(\text{Secchi depth}) \quad (2)$$

$$TSI = 9.81 * \ln(\text{Chl-a}) + 30.6 \quad (3)$$

4 Results

For each sampling site, the corresponding pixel on the atmospherically corrected and normalized satellite image was identified, and its band values were used to generate the band combinations (band differences or ratios). Such calculated band combinations and single bands together with the associated in situ measurement of a given water quality parameter form a match-up pair. For all match-up pairs, three quarters of them are used as the training set for calibrating the water quality parameter retrieval models. The remaining match-up pairs were used as the independent testing set for model accuracy assessment. Table 5 lists the total number of match-up pairs for each water quality parameter with respect to each satellite image source. The corresponding sizes of training and testing data set are also listed in Table 5.

Table 5. Total number of match-up pairs and size of training and testing sets for retrieving turbidity (NTU), Secchi depth (m), and Chl-a ($\mu\text{g/L}$) from Landsat 8 or Sentinel-2 image data.

Satellite	Water Quality Parameter	Training Size	Testing Size	Total Match-Up Pairs
Landsat 8	Turbidity	77	25	102
Landsat 8	Secchi depth	70	23	93
Landsat 8	Chl-a	73	24	97
Sentinel-2	Turbidity	25	9	34
Sentinel-2	Secchi depth	23	7	30
Sentinel-2	Chl-a	27	8	35

4.1 Results from Landsat 8 data

From Band 1 to Band 7 of the preprocessed Landsat 8 images, 21 band differences and 21 band ratios were calculated. In addition to the seven single bands, 49 independent variables were generated. The forward stepwise regression tested the addition of each variable and added the one that yields the most significant improvement of the fit. This process is repeated until no statistically significant improvement can be achieved by inclusion of any variable. The stepwise regression results output best-fit regression models that include an increasing number of independent variables. Among them, the best multiple regression model that includes two independent variables was chosen. For each water quality parameter, raw and log-transformed values were separately used as the dependent

variable, giving rise to two best compact models. Both models in terms of coefficient of determination (R^2) were compared, and the one that had greater R^2 value was selected.

Based on their respective training data sets, the calibrated retrieval models for each water quality parameter are shown below:

$$\text{Turbidity} = (B4-B2) * 0.236 + (B2/B4) * 45.308 - 38.860 \quad (4)$$

$$\log_{10}(\text{Secchi depth}) = (B4-B2) * (-0.002) + B1 * (-0.0004) + 0.1236 \quad (5)$$

$$\log_{10}(\text{Chl-a}) = (B3/B4) * (-0.659) + (B1-B2) * 0.011 + (B3-B1) * 0.003 + 1.027 \quad (6)$$

It was identified that the optimal band combinations for turbidity retrieval are the difference and ratio between red band (B4) and blue band (B2) with $R^2 = 0.643$. Band difference B4-B2 and ultra-blue band B1 explained the most variation of log-transformed Secchi depth ($R^2 = 0.524$). With respect to Chl-a retrieval, none gave satisfactory results ($R^2 \leq 0.5$) when including only two independent variables. Therefore, it was decided to expand the Chl-a retrieval model to include three explanatory variables. Green-red band ratio (B3/B4), green-blue band difference (B3-B1), and difference between two blue bands (B1-B2) are significantly correlated to log-transformed Chl-a concentrations with $R^2 = 0.501$.

It was also found that bands or band combinations were correlated with Secchi depth or Chl-a in a weaker relationship in comparison with the correlation to turbidity given the same model size of two independent variables.

The independent testing sets were used to validate the calibrated water quality parameter retrieval models. The statistical metrics used were Pearson's correlation coefficient (Pearson's r) and root mean square error (RMSE) defined in the following equations:

$$r = \frac{n \sum_{i=1}^n WQP_{pred}^i WPC_{obs}^i - \sum_{i=1}^n WQP_{pred}^i \sum_{i=1}^n WPC_{obs}^i}{\sqrt{n \sum_{i=1}^n (WQP_{pred}^i)^2 - (\sum_{i=1}^n WQP_{pred}^i)^2} \sqrt{n \sum_{i=1}^n (WPC_{obs}^i)^2 - (\sum_{i=1}^n WPC_{obs}^i)^2}} \quad (7)$$

$$RMSE = \sqrt{\frac{\sum_{i=1}^n (WQP_{pred}^i - WPC_{obs}^i)^2}{n}} \quad (8)$$

where

i	=	ID of the sampling point in the test set
n	=	size of the testing set
WQP_{pred}^i	=	predicted value of the concerned water quality parameter for sampling point i
WPC_{obs}^i	=	actual measurement of the concerned water quality parameter for sampling point i .

Figure 4 shows the scatterplots of estimates versus in situ measurements of each water quality parameter using the Landsat 8 testing data set. The Pearson's r between estimated and actual turbidity is 0.797, and the RMSE is 3.82 NTU. For Secchi depth, the Pearson's r between estimates and actual measurements is 0.709, and the prediction RMSE is 0.26 m. As shown in Figure 4(a) and Figure 4(b), sampling points in the testing set generally fall around the diagonal line. Contrarily, the estimated Chl-a concentrations were not well correlated with actual Chl-a measurements with a moderate Pearson's r of 0.553. In Figure 4(c), testing points are scattered far away from the diagonal line, and the predicted RMSE is as large as 6.17 $\mu\text{g/L}$. Chl-a values are heavily overestimated when actual Chl-a concentrations are lower than 15 $\mu\text{g/L}$ and they are underestimated when actual Chl-a concentrations are high ($>15 \mu\text{g/L}$). The underestimation is also evident in Figure 4(a) when in situ measured turbidity is higher than 10 NTU. Equivalently, Secchi depths were overestimated when field Secchi depth measurements are shallower than 0.8 m as shown in Figure 4(b). Both the turbidity and Secchi depth retrieval models tend to underestimate the water clarity when turbidity is high (>10 NTU) or Secchi depth is low (< 0.8 m).

Figure 4. Estimated turbidity (NTU), Secchi depth (m), and Chl-a ($\mu\text{g/L}$) from Landsat 8 data compared with in situ measurements using the testing data set.

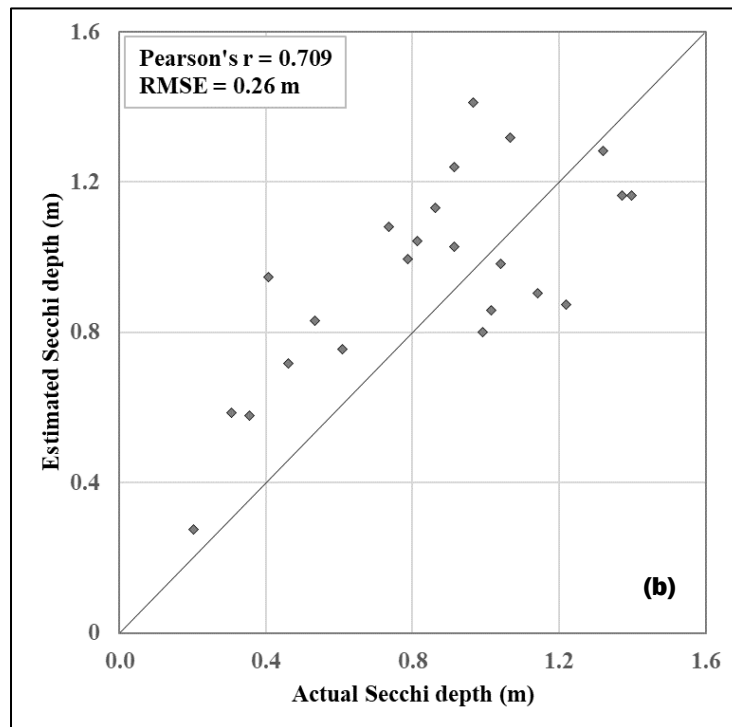
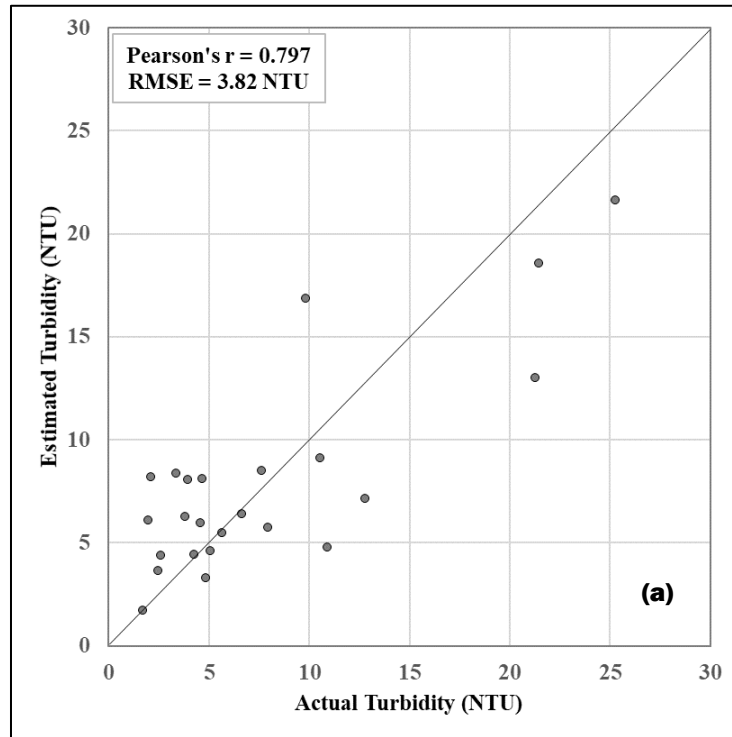
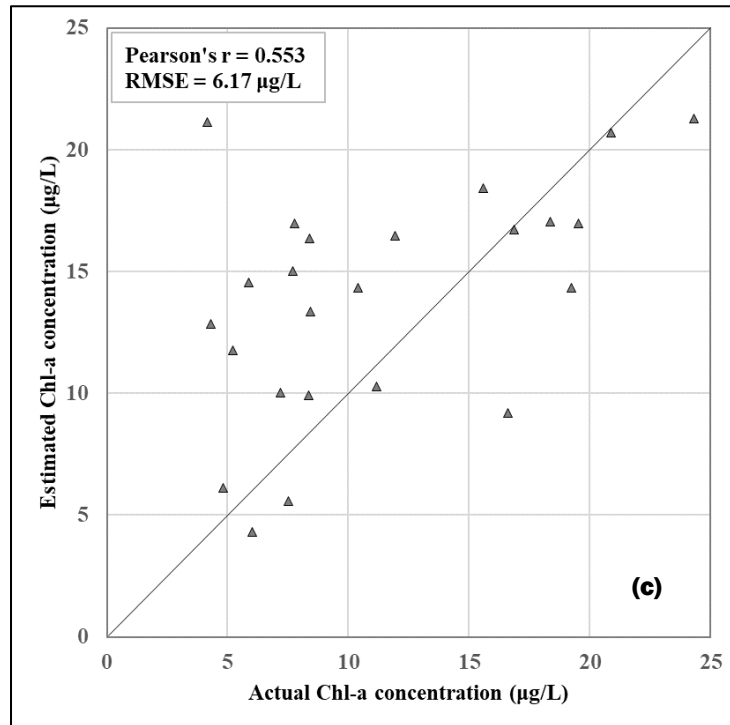


Figure 4. Continued.



4.2 Results from Sentinel-2 data

The nine atmospherically corrected Sentinel-2 bands (Band 1- Band 8a), their band difference, and band ratio combinations constitute 81 independent variables. By performing forward stepwise linear regression on the training data sets, three water quality parameter retrieval models were separately determined:

$$\text{Turbidity} = (B5) * 0.033 + (B8/B8A) * 8.327 - 9.845 \quad (9)$$

$$\log_{10}(\text{Secchi depth}) = (B5) * (-0.001) + (B5/B8A) * (-0.088) + 0.276 \quad (10)$$

$$\text{Chl-a} = (B2-B5) * 0.051 + (B5/B6) * (-1.189) + 11.018 \quad (11)$$

The R^2 of turbidity, Secchi depth, and Chl-a retrieval models are 0.832, 0.812, and 0.836, respectively. Sentinel-2 red-edge band B5 and the ratio of near infrared (NIR) bands B8 to B8A largely explained the variation of actual turbidity measurements ($R^2 = 0.832$). B5 also acted as an important explanatory variable for log-transformed Secchi depth, only with negative coefficients. Inclusion of B5 and B5/B8A explained 81.2% variation of log-transformed Secchi depth. The variation of Chl-a concentration measured in situ was very well modeled by two band combinations which are B2-B5,

difference between blue and red edge band, and B5/B6, ratio of two red edge bands. The three retrieval models have similarly good performances with R^2 greater than 0.80. The prediction accuracies of calibrated models for retrieving turbidity, Secchi depth, and Chl-a were analyzed using the separate testing data sets in terms of Pearson's r and RMSE (Figure 5).

Figure 5. Estimated turbidity (NTU), Secchi depth (m), and Chl-a ($\mu\text{g/L}$) from Sentinel-2 data compared with *in situ* measurements using the testing data set.

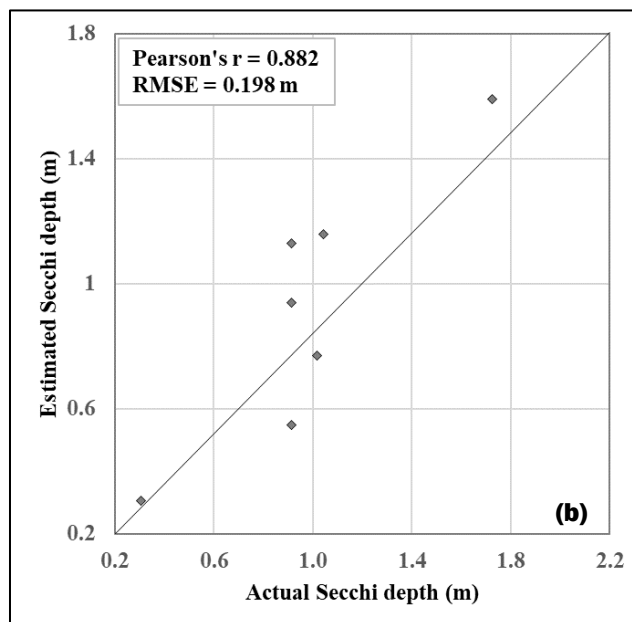
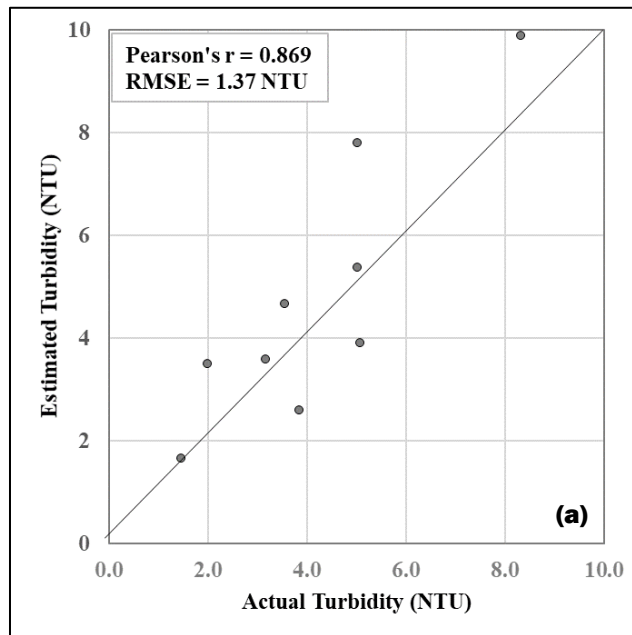
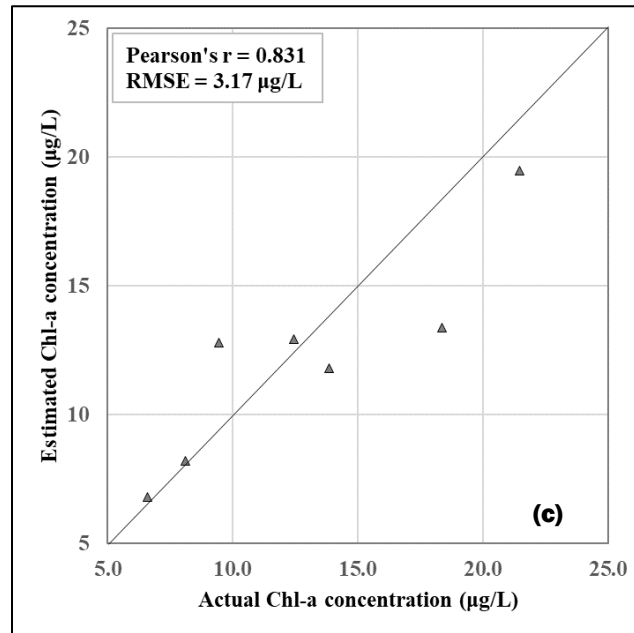


Figure 5. Continued.



As shown in Figure 5, Pearson's r between estimated turbidity and actual turbidity measurements is 0.869, and the prediction RMSE is 1.37 NTU. For Secchi depth, the Pearson's r is 0.882 between estimates and actual values, and the RMSE is 0.198 m. Estimated Chl-a concentrations displayed a strong correlation relationship with actual Chl-a measurements with Pearson's $r = 0.831$ and $RMSE = 3.17 \mu\text{g/L}$. Testing points in Figure 5 located close to the diagonal line showed the excellent agreement between estimated water quality parameters and their actual in situ measurements.

4.3 Spatial pattern of lakes' trophic state

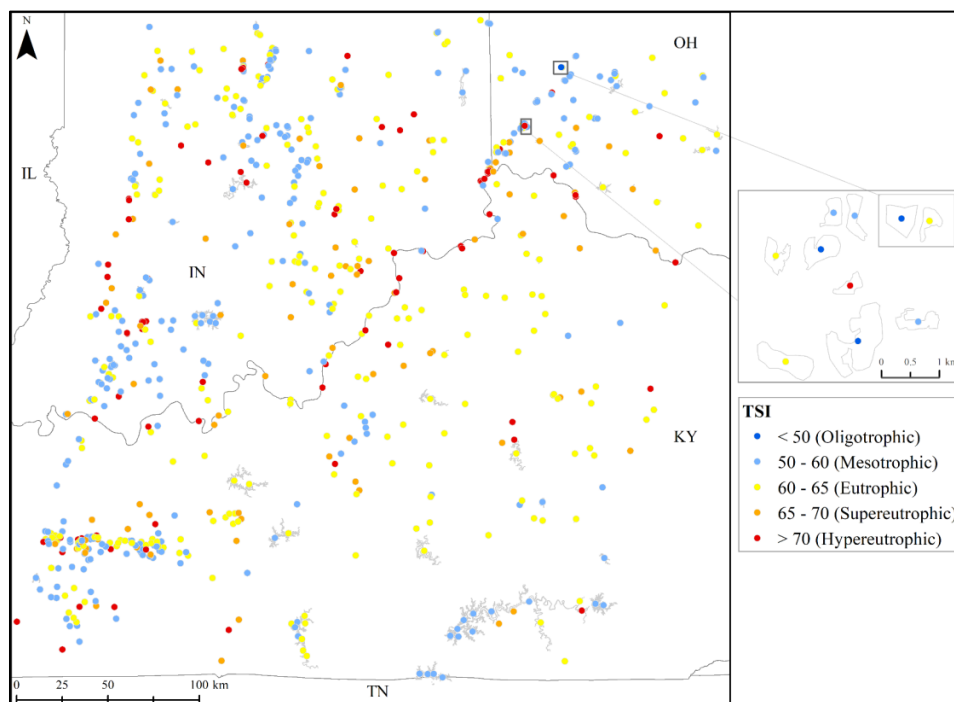
Landsat 8 launched 2 years earlier than Sentinel-2 offered better coverage of the study area in the space and time domain. In this research, Secchi depth derived from time-series Landsat 8 images is used to calculate the TSI based on which the trophic state of lakes were determined and the spatial pattern and temporal variability of lakes' trophic state were analyzed. The TSI of lakes were calculated from derived $\log_{10}(\text{Secchi depth})$ using the equation below:

$$TSI = 60 - 14.41 * (\log_{10}(\text{Secchi depth}) / 0.434) \quad (12)$$

Using Landsat 8 images free of clouds, the average TSI of every studied lake in the Ohio/Indiana/Kentucky region in 2017 was classified and

mapped in Figure 6, following the trophic classification systems in the literature (Crossetti and Bicudo 2008; Kratzer and Brezonik 1981). Water quality conditions are relatively stable in late summer (McCullough et al. 2012), so it was decided to use images acquired in the month of September to calculate and map the lakes' trophic state index. As shown in Figure 6, each lake or reservoir is represented by a circle, and the filled color represents the average trophic state of that lake.

Figure 6. TSI of lakes in September 2017.



The 845 lakes in the study area were grouped into five classes, which are oligotrophic, mesotrophic, eutrophic, supereutrophic, and hypereutrophic. The classification scheme, the total number of lakes, and the percentage of lakes in each class are listed in Table 6. According to Table 6, only a tiny fraction of lakes (0.4%) in the study area have TSI less than 50, and all of the three oligotrophic lakes are located in southwest Ohio (Figure 6). Approximately, 75.2% of the lakes are classified as mesotrophic (40.1%) or eutrophic state (35.1%) whereas the remaining 24.4% of the lakes were identified to be supereutrophic (12.0%) or hypereutrophic (12.4%). There is no apparent spatial correlation in terms of lakes' TSI, but lakes in southern Kentucky tend to have lower TSI values compared with lakes in the north part of Kentucky. It can be seen in Figure 6 that mesotrophic lakes (light blue) in Kentucky are clustered in the south, and most of the lakes in northern Kentucky were in the eutrophic state (yellow).

Table 6. Trophic state classification of 845 lakes in the study area.

TSI	Classification	Number of lakes	Percentage (%)
< 50	Oligotrophic	3	0.4
50-60	Mesotrophic	339	40.1
60-65	Eutrophic	297	35.1
65-70	Supereutrophic	101	12.0
>70	Hyper-eutrophic	105	12.4

The statistics of TSI for this tri-state region in September 2017 were reported in Table 7. Based on Table 7, lakes in the Ohio region have the lowest mean TSI of 60.9, and they also exhibited less variation demonstrated by the smaller standard deviation (STD) compared with the lakes in the Indiana area. TSI of lakes in the Indiana region varies significantly, and it can reach as high as 153.4. Referring to Table 6, the average trophic state in this tri-state area was eutrophic.

Table 7. Summary of lakes' TSI in September 2017.

Region	TSI			
	Min	Max	Mean	STD
KY	51.2	122.5	63.4	7.7
IN	51.2	153.4	63.8	9.6
OH	47.6	101.1	60.9	8.2

The average TSI and classification results of 12 USACE-monitored lakes in the study area are listed in Table 8.

Table 8. TSI and classification of 12 USACE lakes in September 2017.

State	Year	2017	
	Lakes	TSI	Classification
KY	Barren River Lake	56.9	Mesotrophic
	Green River Lake	60.1	Eutrophic
	Nolin River Lake	55.9	Mesotrophic
	Rough River Lake	60.3	Eutrophic
	Taylorsville Lake	61.5	Eutrophic

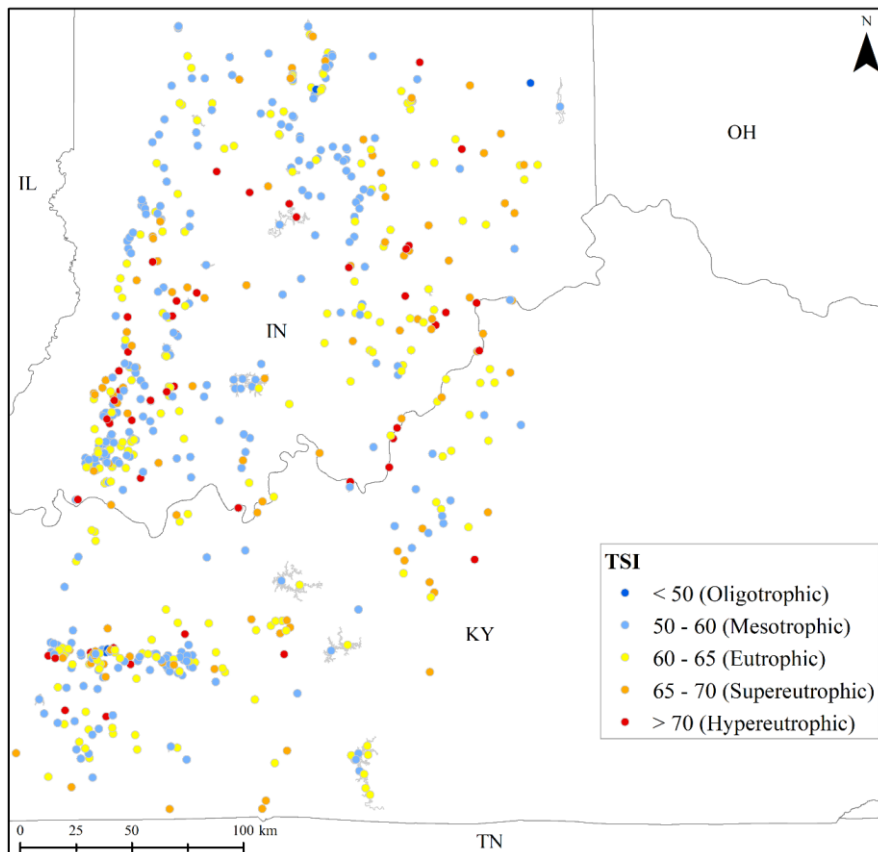
Table 8. Continued.

State	Year	2017	
	Lakes	TSI	Classification
IN	Brookville Lake	56.4	Mesotrophic
	Cagles Mill Lake	60.0	Eutrophic
	Monroe Lake	64.6	Eutrophic
	Patoka Lake	55.9	Mesotrophic
OH	Caesar Creek Lake	58.0	Mesotrophic
	West Fork Lake	67.5	Supereutrophic
	Harsha Lake	60.9	Eutrophic

4.4 Temporal variability of lakes' trophic state

To analyze the temporal variability of lakes' trophic state, the TSI of lakes in September 2013 was also mapped (Figure 7).

Figure 7. TSI of lakes in September 2013.



Note that there are no cloud-free images for Path 20 (Row 33 and 34) in September 2013 or September 2014. To map the TSI of lakes in Path 20, Landsat 8 images acquired in September 2015 (Figure 8) were used. The temporal variability of lakes' TSI in the tri-state region are listed in Table 9. From 2013 to 2017, the minimum, maximum, and STD of TSI in Indiana lakes largely increased. For lakes in southwest Ohio, there was no obvious change except that the maximum TSI increased from 2015 to 2017. The minimum TSI of lakes in Kentucky increased from 2013 to 2017 while the maximum TSI slightly reduced. On average, despite the strong temporal variation in terms of the TSI range (~45.5%) and STD (~22.7%), the mean TSI displayed no significant change (<1.6%). The mean trophic state remain the same (eutrophic) from 2013 to 2017 or from 2015 to 2017.

Figure 8. TSI of lakes in September 2015.

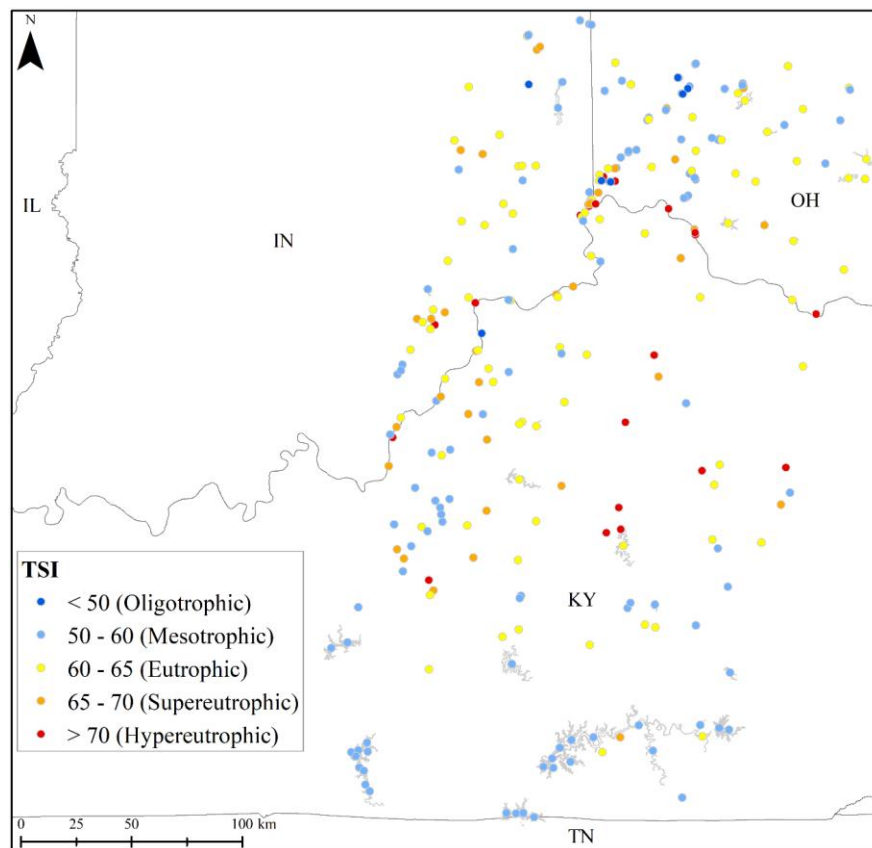


Table 9. Summary of lakes' TSI from different years.

Region	TSI in September					TSI in September 2017			
	Year	Min	Max	Mean	STD	Min	Max	Mean	STD
IN (Path 21)	2013	46.9	112.8	62.8	7.3	51.2	153.4	63.8	9.6
KY (Path 21)	2013	45.8	100.1	62.8	6.6	52.4	91.2	61.8	5.6
KY (Path 20)	2015	52.2	122.4	62.1	7.7	51.2	97.2	62.4	5.5
OH (Path 20)	2015	46.1	78.1	60.8	7.1	47.6	101.1	60.9	8.2

The September TSI of USACE lakes in the study area from different years is listed in Table 10. Most of the USACE-monitored lakes remained the same trophic state or had slightly decreased trophic state index values from 2013 to 2017 except that Green River Lake and West Fork Lake had higher TSI in 2017 compared with that in 2015.

Table 10. TSI and classification of 12 USACE lakes from different years.

State	Lakes	Year	September		September 2017	
			TSI	Classification	TSI	Classification
KY	Barren River Lake	2013	60.8	Eutrophic	59.3	Mesotrophic
	Green River Lake	2015	58.5	Mesotrophic	60.1	Eutrophic
	Nolin River Lake	2013	58.7	Mesotrophic	58.4	Mesotrophic
	Rough River Lake	2013	60.1	Eutrophic	61.4	Eutrophic
	Taylorsville Lake	2015	62.1	Eutrophic	61.5	Eutrophic
IN	Brookville Lake	2013	58.6	Mesotrophic	57.5	Mesotrophic
	Cagles Mill Lake	2013	60.7	Eutrophic	60.0	Eutrophic
	Monroe Lake	2013	64.9	Eutrophic	64.6	Eutrophic
	Patoka Lake	2013	58.2	Mesotrophic	58.8	Mesotrophic
OH	Caesar Creek Lake	2015	61.1	Eutrophic	58.0	Mesotrophic
	West Fork Lake	2015	64.1	Eutrophic	67.5	Supereutrophic
	Harsha Lake	2015	60.3	Eutrophic	60.9	Eutrophic

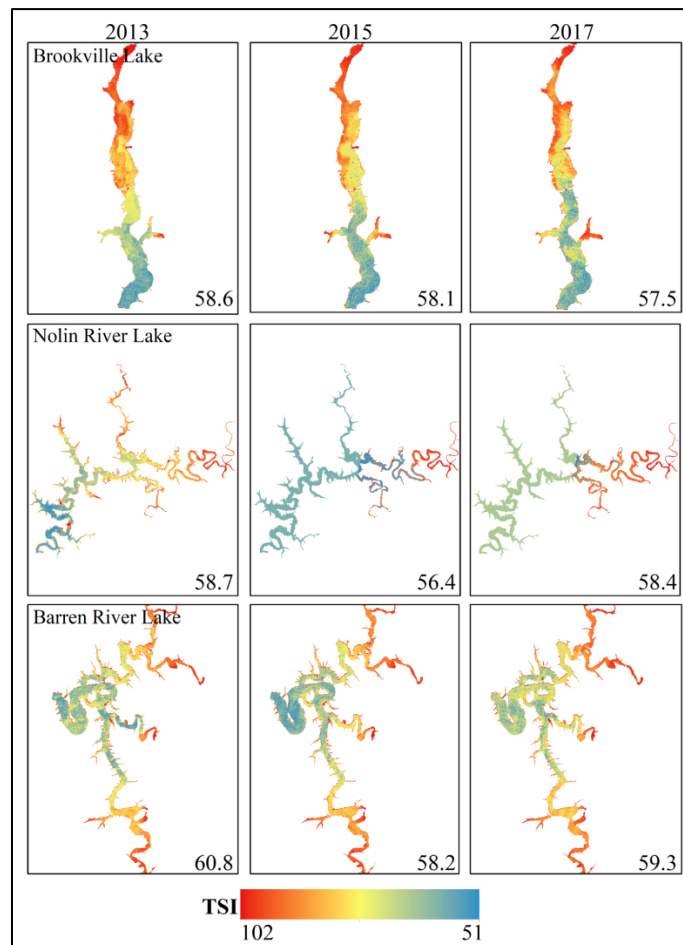
4.5 TSI in individual lakes

Among the 12 USACE lakes, Brookville Lake, Nolin River Lake, and Barren River Lake are situated in the overlapping area of Path 20 and Path 21, so they have TSI maps in all the 3 years. The TSI maps of the three lakes,

respectively, in September 2013, September 2015, and September 2017 are shown in Figure 9.

It is clear that the main stream, together with the upper reaches of the small feeder creeks, often have much higher TSI values than the lake water near the dam (downstream). Lake water in the upstream basin also tends to have greater TSI values compared with lake water in the downstream basin. Brookville Lake exhibited less temporal variability in terms of the TSI values compared with Nolin River Lake and Barren River Lake. From 2013 to 2015, the average TSI of Nolin River Lake reduced to 56.4, and in 2017, it increased to 58.4, very close to the average TSI value in 2013, which is 58.7. Overall, the three lakes' average TSI varied slightly ($< 2.5\%$) from 2013 to 2017.

Figure 9. TSI of Brookville Lake, Rough River Lake, and Barren River Lake in September 2013, September 2015, and September 2017 (mean TSI shown in the right bottom corner).



5 Discussion

Examining the stepwise regression results from Landsat 8 and Sentinel-2 images, it is found that red band (B4 of Landsat 8 OLI or B5 of Sentinel-2 MSI) plays an important role for estimating turbidity and Secchi depth from remotely sensed imagery. It is also found that turbidity and Secchi depth retrieval models commonly share one independent variable that has a positive coefficient in one model and a negative coefficient in the other model. This makes sense because turbidity is strongly and inversely related to Secchi depth. Turbidity, in comparison with Chl-a, can be readily derived from satellite imagery due to the strong backscattering of suspended solids in the red and NIR regions.

Landsat 8 imagery has limited performance for estimating Chl-a concentration mainly because of its band configuration. Chl-a exhibits a unique spectral signature with strong absorptions in the blue (~433 nm) and red (~686 nm) wavelengths and high reflectance in the green (~550 nm) and NIR (~715 nm) spectral regions. Chl-a in inland waters does not co-vary with total suspended solids or colored dissolved organic matter. Empirical algorithms utilizing red and NIR bands for Chl-a retrieval often outperform green and blue band based empirical algorithms resulting from the overlapping and uncorrelated absorption by other water quality parameters in the blue-green spectral region. Landsat 8 has only one NIR band (B5, 850-880 nm), and this band does not correspond to the signature band of Chl-a. In addition, the spectral information of Chl-a may be masked due to the wide widths of Landsat 8 OLI VNIR bands. Thus, it is not surprising to find the unsatisfactory performance of Chl-a retrieval algorithms calibrated from Landsat 8 training data set, especially when Chl-a are highly concentrated.

Sentinel-2, conversely, has more appropriate placement of spectral bands for the retrieval of water quality parameters. It has three narrow red edge bands B5, B6, and B7, with central wavelengths of ~704, ~740, and ~780 nm, respectively, that are appropriate for Chl-a estimation. Two NIR bands (B8 and B8a) also enhanced its potential for turbidity retrieval. Consequently, water quality parameter retrieval models based on the Sentinel-2 data have much better prediction accuracy compared with those calibrated from Landsat 8 data. Comparing turbidity estimation accuracy between Sentinel-2 and Landsat 8, the Pearson's r was 0.869 versus 0.797, and RMSE was 1.37 NTU versus 3.82 NTU. The Pearson's r

was improved from 0.709 (Landsat 8) to 0.882 (Sentinel-2), and RMSE was reduced from 0.264 m (Landsat 8) to 0.198 m (Sentinel-2) for Secchi depth retrieval. In terms of Chl-a prediction, the Sentinel-2 based retrieval model yielded a much higher Pearson's r of 0.831 compared to 0.553 from the Landsat 8 based retrieval model. The RMSE was largely reduced from 6.17 $\mu\text{g/L}$ to 3.17 $\mu\text{g/L}$. However, because Sentinel-2 is relatively new, the available number of training points is much smaller compared with Landsat 8.

Landsat 8 has better spatial and temporal coverage for the study area due to the longer operation period. Therefore, Landsat 8-based Secchi depth estimates were used to derive and map trophic state of lakes in this region. To make the TSI from different lakes or from different years comparable, images acquired in the same month (September) were used to calculate the TSI. Based on the analysis, most lakes (~75%) in the study area were mesotrophic or eutrophic, and the average trophic state was eutrophic in 2017. Lakes in the south of Kentucky tend to have smaller TSI values than lakes in northern Kentucky. Temporally, TSI of lakes in Indiana region experienced an increase in terms of the minimum, maximum, and STD values. For lakes in Kentucky, the minimum TSI increased and the maximum TSI reduced since 2013. Lakes in southwest Ohio area had no significant change in TSI statistics. Despite the strong temporal variability in TSI range and STD, the average TSI in this tri-state area displayed no significant change (<1.6%). The average trophic state of each sub-region remained eutrophic from 2013 to 2017.

For the 12 USACE lakes in the study area, most of them had the same trophic state or slightly decreased trophic state index from 2013 to 2017, except Green River Lake and West Fork Lake. USACE lakes including Brookville Lake, Nolin River Lake, and Barren River Lake have TSI maps in 2013, 2015, and 2017, respectively. When zooming into the three individual lakes, it is found that lake water in the upstream basin was more eutrophic than water in the downstream basin and that the main stream and tributaries often had large TSI values. This may be explained by the fact that inflows usually come with a high load of nutrients and sediments, which is preferable for biological activity (e.g., algae growth) in the water. After examining the average TSI of each lake in the 3 years, a slight variation (< 2.5%) in average TSI from 2013 to 2017 was identified. For Barren River Lake and Nolin River Lake, the average TSI decreased from 2013 to 2015 and then increased in 2017 to a value close to that in 2013.

Derived Secchi depth was used to calculate the TSI because the Chl-a retrieval model calibrated for Landsat 8 did not perform reasonably well. In future research, Sentinel-2 data and the corresponding Chl-a retrieval model will be used to map and analyze the trophic state of lakes in this region. The results will also be compared or cross validated with those obtained from Landsat 8 data.

6 Conclusion

This research evaluated Landsat 8 and Sentinel-2 imagery for regional lake water quality assessment and analyzed the spatial pattern and temporal variability of lakes' trophic state in the Ohio/Kentucky/Indiana region. Combining atmospherically corrected satellite images with coincident water quality data from the USACE Louisville District Water Quality Team and the USEPA Water Quality Portal, stepwise linear regression was used to calibrate empirical models for retrieval of water quality parameters, including turbidity, Secchi depth, and Chl-a.

Landsat 8 multispectral imagery is well suited for regional assessment of turbidity and Secchi depth, but the low spectral resolution and the lack of appropriate red-edge bands limits its capability in assessing Chl-a concentration. The spatial resolution of Landsat 8 allows lakes larger than 90,000 m² to be assessed. Using time-series Landsat 8 images and a predefined Secchi depth retrieval model, the TSI of lakes in the tri-state region in 2013, 2015, and 2017 was computed. Approximately 75% of the lakes in the study area were identified as mesotrophic to eutrophic in 2017, and there was only a very small number of lakes situated in southwest Ohio with TSI values less than 50 (oligotrophic). From 2013 to 2017, the average TSI in this tri-state area displayed no significant change (retaining an average eutrophic state); however, the TSI range and STD of lakes in Indiana region largely increased. In an individual lake, water in the downstream basin had less TSI values than water in the upstream basin, and area where a river or stream flowing into the lake had high TSI values.

The positions and widths of Sentinel-2 spectral bands allow the accurate retrieval of turbidity, Secchi depth, and Chl-a concentration. Furthermore, taking into account the more frequent revisits and finer spatial resolution, Sentinel-2 MSI is a more appropriate sensor for monitoring inland water quality at a regional scale when sufficient training points are available and the desired spatial and temporal coverage can be satisfied.

References

- Adler-Golden, S., A. Berk, L. Bernstein, S. Richtsmeier, P. Acharya, M. Matthew, G. Anderson, C. Allred, L. Jeong, and J. Chetwynd. 1998. "FLAASH, a MODTRAN4 Atmospheric Correction Package for Hyperspectral Data Retrievals and Simulations." *Proc. 7th Ann. JPL Airborne Earth Science Workshop*, 9-14.
- Beck, R., S. Zhan, H. Liu, S. Tong, B. Yang, M. Xu, Z. Ye, Y. Huang, S. Shu, and Q. Wu. 2016. "Comparison of Satellite Reflectance Algorithms for Estimating Chlorophyll-a in a Temperate Reservoir Using Coincident Hyperspectral Aircraft Imagery and Dense Coincident Surface Observations." *Remote Sensing of Environment* 178: 15-30.
- Blondeau-Patissier, D., J. F. Gower, A. G. Dekker, S. R. Phinn, and V. E. Brando. 2014. "A Review of Ocean Color Remote Sensing Methods and Statistical Techniques for the Detection, Mapping and Analysis of Phytoplankton Blooms in Coastal and Open Oceans." *Progress in Oceanography* 123: 123-144.
- Carlson, R. E. 1977. "A Trophic State Index for Lakes." *Limnology and Oceanography* 22: 361-369.
- Chen, Z., F. E. Muller-Karger, and C. Hu. 2007. "Remote Sensing of Water Clarity in Tampa Bay." *Remote Sensing of Environment* 109: 249-259.
- Crossetti, L. O., and C. E. d. M. Bicudo. 2008. "Phytoplankton as a Tool in a tropical Urban Shallow Reservoir (Garças Pond): The Assemblage Index Application." *Hydrobiologia* 610: 161-173.
- Dodds, W. K., J. R. Jones, and E. B. Welch. 1998. "Suggested Classification of Stream Trophic State: Distributions of Temperate Stream Types by Chlorophyll, Total Nitrogen, and Phosphorus." *Water Research* 32: 1455-1462.
- Dogliotti, A., K. Ruddick, B. Nechad, D. Doxaran, and E. Knaeps. 2015. "A Single Algorithm to Retrieve Turbidity from Remotely-Sensed Data in All Coastal and Estuarine Waters." *Remote Sensing of Environment* 156: 157-168.
- Drusch, M., U. Del Bello, S. Carlier, O. Colin, V. Fernandez, F. Gascon, B. Hoersch, C. Isola, P. Laberinti, and P. Martimort. 2012. "Sentinel-2: ESA's Optical High-Resolution Mission for GMES Operational Services." *Remote Sensing of Environment* 120: 25-36.
- Effler, S. 1988. "Secchi Disc Transparency and Turbidity." *Journal of Environmental Engineering* 114: 1436-1447.
- El-Serehy, H. A., H. S. Abdallah, F. A. Al-Misned, S. A. Al-Farraj, and K. A. Al-Rasheid. 2018. "Assessing Water Quality and Classifying Trophic Status for Scientifically Based Managing the Water Resources of the Lake Timsah, the Lake with Salinity Stratification along the Suez Canal." *Saudi Journal of Biological Sciences* 25: 1247-1256.

- Fuller, L. M., S. S. Aichele, and R. J. Minnerick. 2004. *Predicting Water Quality by Relating Secchi-Disk Transparency and Chlorophyll-a Measurements to Satellite Imagery for Michigan Inland Lakes, August 2002*. US Department of the Interior, US Geological Survey.
- Fuller, L. M., and R. J. Minnerick. 2007. "Predicting Water Quality by Relating Secchi-Disk Transparency and Chlorophyll-a Measurements to Landsat Satellite Imagery for Michigan inland lakes, 2001-2006." US Geological Survey.
- Harrington, J. A., F. R. Schiebe, and J. F. Nix. 1992. "Remote Sensing of Lake Chicot, Arkansas: Monitoring Suspended Sediments, Turbidity, and Secchi Depth with Landsat MSS Data." *Remote Sensing of Environment* 39: 15-27.
- Kloiber, S. M., P. L. Brezonik, and M. E. Bauer. 2002a. "Application of Landsat Imagery to Regional-Scale Assessments of Lake Clarity." *Water Research* 36: 4330-4340.
- Kloiber, S. M., P. L. Brezonik, L. G. Olmanson, and M. E. Bauer. 2002b. "A Procedure for Regional Lake Water Clarity Assessment Using Landsat Multispectral Data." *Remote Sensing of Environment* 82: 38-47.
- Kratzer, C. R., and P. L. Brezonik. 1981. "A Carlson-Type Trophic State Index for Nitrogen in Florida Lakes." *Journal of the American Water Resources Association* 17: 713-715.
- Kutser, T., D. C. Pierson, K. Y. Kallio, A. Reinart, and S. Sobek. 2005. "Mapping Lake CDOM by Satellite Remote Sensing." *Remote Sensing of Environment* 94: 535-540.
- Martin, R., E. Boebel, R. Dunst, O. Williams, M. Olsen, R. Merideth, Jr., and F. Scarpace. 1983. "Wisconsin Lakes—A Trophic Assessment Using Landsat Digital Data." *Wisconsin Lake Classification Survey Project S, 536601*, 294.
- McCullough, I. M., C. S. Loftin, and S. A. Sader. 2012. "Combining Lake and Watershed Characteristics with Landsat TM Data for Remote Estimation of Regional Lake Clarity." *Remote Sensing of Environment* 123: 109-115.
- Olmanson, L. G., M. E. Bauer, and P. L. Brezonik. 2008. "A 20-Year Landsat Water Clarity Census of Minnesota's 10,000 Lakes." *Remote Sensing of Environment* 112: 4086-4097.
- Olmanson, L. G., P. L. Brezonik, and M. E. Bauer. 2011. "Evaluation of Medium to Low Resolution Satellite Imagery for Regional Lake Water Quality Assessments." *Water Resources Research* 47.
- Olmanson, L. G., P. L. Brezonik, and M. E. Bauer. 2015. "Remote Sensing for Regional Lake Water Quality Assessment: Capabilities and Limitations of Current and Upcoming Satellite Systems." *Advances in Watershed Science and Assessment*. Springer.
- Olmanson, L. G., P. L. Brezonik, J. C. Finlay, and M. E. Bauer. 2016. "Comparison of Landsat 8 and Landsat 7 for Regional Measurements of CDOM and Water Clarity in Lakes." *Remote Sensing of Environment* 185: 119-128.

- Ritchie, J. C., P. V. Zimba, and J. H. Everitt. 2003. "Remote Sensing Techniques to Assess Water Quality." *Photogrammetric Engineering & Remote Sensing* 69: 695-704.
- Vidot, J., and R. Santer. 2005. "Atmospheric Correction for Inland Waters—Application to SeaWiFS." *International Journal of Remote Sensing* 26: 3663-3682.
- Watanabe, F., E. Alcantara, T. Rodrigues, L. Rotta, N. Bernardo, and N. Imai. 2017. "Remote Sensing of the Chlorophyll-a Based on OLI/Landsat-8 and MSI/Sentinel-2A (Barra Bonita Reservoir, Brazil)." *Anais da Academia Brasileira de Ciências*, 0-0.
- Xu, M., H. Liu, R. Beck, J. Lekki, B. Yang, S. Shu, E. L. Kang, R. Anderson, R. Johansen, and E. Emery. 2018. "A Spectral Space Partition Guided Ensemble Method for Retrieving Chlorophyll-a Concentration in Inland Waters from Sentinel-2A Satellite Imagery." *Journal of Great Lakes Research* 45(3): 454-465.
- Xu, M., H. Liu, R. Beck, J. Lekki, B. Yang, S. Shu, Y. Liu, T. Benko, R. Anderson, R. Tokars, and R. Johansen. 2019. "Regionally and Locally Adaptive Models for Retrieving Chlorophyll-a Concentration in Inland Waters From Remotely Sensed Multispectral and Hyperspectral Imagery." *IEEE Transactions on Geoscience and Remote Sensing*. Piscataway, NJ: IEEE.

Acronyms and Abbreviations

Chl-a	chlorophyll-a
BOA	bottom-of-atmosphere
ENVI	Environment for Visualizing Images
FLAASH	Fast Line-of-sight Atmospheric Analysis of Spectral Hypercubes
MSI	multispectral instrument
NIR	near infrared
NTU	nephelometric turbidity units
OLI	Operational Land Imager
RMSE	root mean square error
SNAP	Sentinel Application Platform
SNR	signal-to-noise ratio
STD	standard deviation
SWIR	shortwave infrared
TIRS	Thermal Infrared Sensor
TOA	top-of-atmosphere
TSI	trophic state index
USACE	United States Army Corps of Engineers
USEPA	United States Environmental Protection Agency
UTM	Universal Transverse Mercator
VNIR	visible and near infrared
WGS84	World Geodetic System 84

REPORT DOCUMENTATION PAGE

Form Approved
OMB No. 0704-0188

The public reporting burden for this collection of information is estimated to average 1 hour per response, including the time for reviewing instructions, searching existing data sources, gathering and maintaining the data needed, and completing and reviewing the collection of information. Send comments regarding this burden estimate or any other aspect of this collection of information, including suggestions for reducing the burden, to Department of Defense, Washington Headquarters Services, Directorate for Information Operations and Reports (0704-0188), 1215 Jefferson Davis Highway, Suite 1204, Arlington, VA 22202-4302. Respondents should be aware that notwithstanding any other provision of law, no person shall be subject to any penalty for failing to comply with a collection of information if it does not display a currently valid OMB control number.
PLEASE DO NOT RETURN YOUR FORM TO THE ABOVE ADDRESS.

1. REPORT DATE November 2019		2. REPORT TYPE Final Report		3. DATES COVERED (From - To)	
4. TITLE AND SUBTITLE Regional Analysis of Lake and Reservoir Water Quality with Multispectral Satellite Remote Sensing Images				5a. CONTRACT NUMBER	
				5b. GRANT NUMBER	
				5c. PROGRAM ELEMENT NUMBER	
6. AUTHOR(S) Min Xu, Hongxing Liu, Richard A. Beck, Molly K. Reif, Erich B. Emery, and Jade L. Young				5d. PROJECT NUMBER	
				5e. TASK NUMBER	
				5f. WORK UNIT NUMBER	
7. PERFORMING ORGANIZATION NAME(S) AND ADDRESS(ES) (see reverse)				8. PERFORMING ORGANIZATION REPORT NUMBER ERDC/EL TR-19-19	
9. SPONSORING/MONITORING AGENCY NAME(S) AND ADDRESS(ES) Aquatic Nuisance Species Research Program US Army Engineer Research and Development Center Environmental Laboratory Vicksburg, MS 39180-6199				10. SPONSOR/MONITOR'S ACRONYM(S) ANSRP	
				11. SPONSOR/MONITOR'S REPORT NUMBER(S)	
12. DISTRIBUTION/AVAILABILITY STATEMENT Approved for public release; distribution is unlimited.					
13. SUPPLEMENTARY NOTES Funding Account Code 96 X 3123; AMSCO Code 008284					
14. ABSTRACT In this research, a time-series of multispectral images acquired by Landsat 8 and Sentinel-2 satellites during 2013-2017 was combined with in situ water quality measurements to examine and analyze the spatial pattern and temporal variation of lake and reservoir water quality in the Ohio/Kentucky/Indiana region within the Louisville District, United States Army Corps of Engineers. Reflectance values at the sampling sites for each lake were used with the in situ data collected within a 7-day time window of satellite overpass to construct empirical models to estimate water quality parameters, including turbidity, Secchi depth, and chlorophyll-a. The analysis indicated that Sentinel-2 outperformed Landsat 8 for retrieving water quality parameters, especially for chlorophyll-a. Due to the better spatial and temporal coverage of Landsat 8 for this tri-state region, the Secchi depth retrieved from the time-series Landsat 8 images was used to create lake trophic state index (TSI) maps in 2013, 2015, and 2017. It was observed that most lakes (~75%) in the study area were in mesotrophic or eutrophic classes in 2017 based on the TSI. From 2013 to 2017, the TSI range and standard deviation of lakes in Indiana region largely increased while the average TSI in this tri-state area varied slightly (<1.6%).					
15. SUBJECT TERMS Environmental management, Multispectral imaging, Remote-sensing images, Reservoirs—Water quality, Water quality management					
16. SECURITY CLASSIFICATION OF:			17. LIMITATION OF ABSTRACT SAR	18. NUMBER OF PAGES 44	19a. NAME OF RESPONSIBLE PERSON Molly Reif
a. REPORT Unclassified	b. ABSTRACT Unclassified	c. THIS PAGE Unclassified			19b. TELEPHONE NUMBER (Include area code) 228-252-1134

7. PERFORMING ORGANIZATION NAME(S) AND ADDRESS(ES) (continued)

Department of Geography
The University of Alabama
513 University Blvd
Tuscaloosa, AL 35487

Department of Geography and Geographic Information Science
University of Cincinnati
Cincinnati, OH 45221

U.S. Army Corps of Engineers, ERDC, JALBTCX
7225 Stennis Airport Rd
Kiln, MS, 39556

U.S. Army Corps of Engineers, Great Lakes and Ohio River Division
550 Main Street
Cincinnati, OH 45202

U.S. Army Corps of Engineers, Louisville District, Water Quality
Louisville, KY 40202